



# Improved Multiphase Flow Rate Models for Chokes in the Algerian HMD Oil Field

Nour ElHouda Tellache<sup>1</sup> · Meriem Waffa Hassen<sup>1</sup> · Mohamed Otmanine<sup>2</sup> · Mohamed Khodja<sup>1</sup>

Received: 11 December 2019 / Accepted: 17 September 2020 / Published online: 6 October 2020  
© King Fahd University of Petroleum & Minerals 2020

## Abstract

Accurate prediction of multiphase flow rate is of prime importance in controlling production of oil fields. Direct measurements using multiphase meters are time-consuming and very costly. On the other hand, none of the published models can be considered as a universal model and most of these models are designated only for the critical flow. The aim of this study is to develop and validate practical models for the Algerian Hassi Messaoud (HMD) oil field covering both critical and subcritical multiphase flows through chokes of naturally flowing and gas lift wells. The new choke models are developed on the basis of the Gilbert model by incorporating the downstream pressure of the choke under the subcritical conditions. A large data set is used to evaluate the new models and to compare their performance with previously published prediction models. These data are divided, for each flow regime, into five selected categories based on the gas–oil ratio and a nonlinear regression algorithm is implemented to validate the new models. The comparison revealed the accuracy of two new models that improved the predicted production rates of the current model of HMD field in 130 wells out of 174 and the sum of absolute differences between the measured and the predicted oil flow rates (SAD) was reduced by 16.68% on 6,786 measurements. For the wells that are assisted with gas lift, the predictability was improved considerably: There was improvement in 85 wells out of 93 and the SAD was reduced by 42.11% on 2,317 measurements.

**Keywords** Oil flow rate · Choke · Multiphase flow · Critical and subcritical flow · HMD

## List of Symbols

|            |   |
|------------|---|
| $Q$        | Gross liquid rate (bbl/day [ $\text{m}^3/\text{h}$ ])           |
| $Q_o$      | Oil flow rate (bbl/day [ $\text{m}^3/\text{h}$ ])               |
| $P_u$      | Wellhead (or upstream) pressure (psig [bar])                    |
| $P_d$      | Flowline (or downstream) pressure (psig [bar])                  |
| $\phi$     | Choke size (1/64 inch [m])                                      |
| GLR        | Gas–liquid ratio (MSCF/BBL)                                     |
| GOR        | Gas–oil ratio (MSCF/BBL [ $\text{sm}^3/\text{m}^3$ ])           |
| $\Delta P$ | Pressure drop across the choke (psig [bar])                     |
| $Q_e$      | Estimated oil flow rate (bbl/day [ $\text{m}^3/\text{h}$ ])     |
| $Q_m$      | Measured oil flow rate (bbl/day [ $\text{m}^3/\text{h}$ ])      |
| SAD        | Sum of absolute differences (bbl/day [ $\text{m}^3/\text{h}$ ]) |
| SD         | Sum of differences (bbl/day [ $\text{m}^3/\text{h}$ ])          |

|                   |                         |
|-------------------|-------------------------|
| RAE               | Relative absolute error |
| RE                | Relative error          |
| $W_i$             | Well $i$                |
| Nb data           | Number of measurements  |
| $a, b, c$ and $d$ | Empirical constants     |

## 1 Introduction

The phenomenon of multiphase flow (liquid and gas) occurs in the wellhead of almost all producing wells. The flow rate of these wells is usually regulated using wellhead chokes. A choke is a restriction in cross sectional area of flow path, restricting flow rate by imposing pressure drop to the producing fluid. There are two main types of chokes: fixed with non-adjustable diameter and variable that allow adjustments to their diameter. Controlling the flow using wellhead chokes prevents reservoir damage by creating a back pressure, maintains the integrity and safety of surface equipment against slugging at high flowing pressures, stabilizes production flow rate and prevents water and gas coning and sand production

✉ Nour ElHouda Tellache  
nour.tellache@gmail.com

<sup>1</sup> Central Directorate Research and Development, Sonatrach, Avenue 1st November, 35000 Boumerdes, Algeria

<sup>2</sup> Production Division, Sonatrach, BP50 Base IRARA, 30500 Hassi Messaoud, Algeria



[1]. Besides controlling the flow rate, the chokes are also used to provide sufficient data for rate estimation. The study of the flow rate of a multiphase mixture through a wellhead choke is a critical part of many important applications in the oil and gas industry including the optimization and control of production, as well as the characterization of reservoirs.

Before calculating the liquid flow rate through chokes, it is necessarily to determine if the flow behavior of the gas–liquid mixture through the choke is critical (sonic) or subcritical (sub-sonic). When the velocity of the fluids flowing across the choke reaches the sonic velocity for the fluid, the flow in the choke is critical. In contrast, the subcritical flow occurs when the velocities of the fluids traversing the choke drop below the sonic velocity of the fluids [2]. Therefore, in the critical flow conditions, the rate is related only to the upstream pressure of the choke and any pressure fluctuations introduced downstream the choke will not affect the rate because these fluctuations can never be transmitted upstream. In the subcritical conditions, however, the flow rate is a function of the downstream pressure of the choke. The wellhead chokes are usually operated under the critical regime in order to achieve stable flow rates and to isolate the reservoir from the frequent perturbations in the surface equipment. Since it is difficult to estimate the local sound speed in the field, the boundary between the two regimes is defined by a pressure ratio of downstream to upstream. The value of the ratio is usually considered in the literature equal to 0.5 [3].

The most accurate tools used to measure the oil well production through wellhead chokes in a multiphase environment are the separators and the multiphase meters [4]. However, these methods are very costly and time-consuming to implement on a field-wide basis [5]. In contrast, it is required to have a quick and an accurate evaluation of the well production in order to optimize the performance of the entire production system. Due to the complexity of the Navier Stokes equations, it is difficult to have an exact evaluation of the oil flow rate of a multiphase mixture through a choke, but several models have been developed with the intention of having an accurate estimation of the oil rate with minimum number of parameters using numerical solutions. These models fall into two main categories: theoretical and empirical [6]. The theoretical models are derived from the mass, momentum and energy balance laws of the fluid across the choke [7]. These models have too many parameters and require fluid properties which may not be available in many fields, and this makes them difficult to apply. The empirical models are limited to special operational conditions including the range of field or experimental data used in their development stage [8]. As a result, these models return acceptable results within the flow conditions upon which they were based, but the accuracy of the estimation decreases when extrapolated to new flow conditions. Although numerous empirical models have been developed for describing

simultaneous liquid and gas flow through wellhead chokes, almost all of them are under the critical conditions, while there are few ones for the subcritical regime. These models are surveyed in the next section.

The objective of the present study is to develop practical and accurate multiphase flow models for predicting the oil production rate through chokes of naturally flowing and gas lift wells under critical and subcritical flow conditions. The developed models extend the Gilbert model [9] to fit the measured data and to handle both flow regimes. The idea of these models is to take into account the downstream pressure of the choke under the subcritical conditions. Based on a large data set collected from the HMD oil field, a nonlinear regression algorithm is used to find out the correlations that best fit the measured data for different ranges of the gas–oil ratio. It should be noted that during the last years in HMD, most of the flows are in the subcritical regime. A comparison between the obtained models and other existing models is done with different error parameters. The proposed models are valid on a wide range of flow variables, especially for high GOR values.

## 2 Related Literature

Over the past six decades, many papers have addressed the prediction of the oil flow rate through wellhead chokes in a multiphase environment either by proposing new models or by conducting a comparison study to test the efficiency of the existing models on a given field. Tangren et al. [10] presented in 1949 the first study that analyses the gas/liquid two-phase flow through a choke under the critical flow conditions. They assumed a homogeneous mixture in which the gas bubbles are so small and uniformly distributed in the liquid that the velocities of the two phases can be considered the same during expansion. This assumption occurs where the liquid is the continuous phase. Gilbert [9] developed in 1954 the most popular multiphase flow model for calculating the liquid flow rate through a choke. He used 268 production test data of the Ten Section field in California for choke sizes between 6/64 and 18/64 inch. This model is valid for the critical flow occurring when the mixture velocities through the choke reach the speed of sound. As seen in the previous section, the speed of sound is known to be reached when the upstream pressure of the choke is at least twice the downstream pressure. Gilbert noted, however, that his model is good when the upstream pressure of the choke is at least 70% greater than the downstream pressure of the choke. This model takes the following from:

$$Q = a \frac{P_u \cdot \phi^b}{GLR^c} \quad (1)$$

**Table 1** Correlation constants for Gilbert-type equations under the critical flow conditions

| Correlation             | <i>a</i> | <i>b</i> | <i>c</i> | References                   |
|-------------------------|----------|----------|----------|------------------------------|
| Gilbert                 | 0.1      | 1.89     | 0.546    | Gilbert [9]                  |
| Baxendell               | 0.104    | 1.93     | 0.546    | Baxendell [30]               |
| Ros                     | 0.05747  | 2.0      | 0.5      | Ros [11]                     |
| Achong                  | 0.2618   | 1.88     | 0.65     | Achong [24]                  |
| Pilehvari               | 0.021427 | 0.313    | 2.11     | Pilehvari [31]               |
| Safar Beiranvand et al. | 0.0328   | 2.275    | 0.586    | Safar Beiranvand et al. [38] |

where  $Q$  (bbl/day), GLR (MSCF/BBL),  $P_u$  (psig) and  $\phi$  (1/64 inch). The correlating exponents of Gilbert [9] are as follows:  $a = 0.1$ ,  $b = 1.89$ ,  $c = 0.546$ . This formula offers the possibility of using the choke as a flow meter; from its pressure readings, the  $Q$  can be estimated once GLR is known, and vice versa. Many subsequent studies and adaptations have emerged on the basis of the study of Gilbert [9]; Table 1 summarizes some of the correlations that have the same form as that of Gilbert [9] but with different constants and variables exponents.

Ros [11] extended the work of Tangren et al. [10] and studied the case in which the gas is the continuous phase. Poettmann and Beck [12] proposed a model in which they introduced some fluid properties. This model is obtained by converting Ros's correlation [11] to graphical forms. Omana [13] also introduced the fluid properties in his model which is obtained by series of laboratory tests for critical two-phase flow of gas–water mixtures. This model is valid for specific ranges of choke size, liquid flow rate and upstream pressure. Ashford and Pierce [14] presented a model that is valid for both critical and subcritical regimes. They derived the model from the energy balance for flowing fluids across a restriction, and they used the specific heat ratio in their derivations. Examples of other well-known models are Sachdeva et al. [2], Perkins [15], Al-Safran and Kelkar [16] and the Hydro model that has been proposed first in [17] and improved later in [18,19]. The reader is referred to Shao et al. [7], Mwa-lyepelo and Stanko [6] and Rastoin et al. [20] for a detailed literature review and a comparison of the latter models.

Al-Attar and Abdul-Majeed [21] conducted a comparison study between three models on 155 well tests, where 20 tests are from the East Baghdad oil field. The overall results showed that the Gilbert model [9] was, in general, more efficient than Poettmann and Beck [12] and Ashford [22] models. The Gilbert model [9] is then revised in two forms to find out the correlations that best fit the measured data from the East Baghdad oil field. Abdul-Majeed and Maha [23] tested the accuracy of eight correlations on 210 well tests with 56 tests from Iraq wells. They found that the Gilbert model [9] seems to perform better especially when the choke size increases followed by Ashford [22] and Ros [11] models. Poettmann and Beck [12] and Ros [11] models yielded better results for

small choke sizes, whereas Achong [24], Al-Attar and Abdul-Majeed [21] and Omana [13] were totally unsatisfactory. Then, four new correlations were developed using multiple regression analysis for different data categories. Elgibaly and Nashawi [25] also tested a number of correlations on 260 well tests: 154 tests under critical regime and 106 tests under subcritical regime. In the critical flow, the correlation based on Gilbert model [9] performed better than two correlations derived from Ashford and Pierce [14] model. For the subcritical flow, the authors developed the model given in Eq. (2), in which they used  $\Delta P$  rather than  $P_u$  in the Gilbert equation [9]. They found that the accuracy of their equation on flow data of Kuwait is closely comparable to the Ashford and Pierce [14] correlation modified by Abdul-Majeed and Aswad [26]. They also evaluated the Ashford and Pierce [14] correlation modified by using the correlations developed by Al-Marhoun [27] and Dranchuk et al. [28] to estimate the PVT properties of the produced fluids. The results showed that this latter model performed better than the former two models. Mirzaei-Paiaman and Salavat [29] used 132 measurements from 15 Persian oil fields. These data include, besides the parameters of the Gilbert model, the gas and oil specific gravities. The authors showed that choke performance is fairly insensitive to the latter two parameters. They also calculated a Gilbert-type correlation based on the data of the Persian oil fields, and they found that their correlation yields statistically better results than those of Gilbert [9], Ros [11], Baxendell [30], Achong [24] and Pilehvari [31]. In summary, Gilbert-type formulae have been developed by many investigators, they appear to be practically more favorable due to their simplicity, and they do not require measurements of many parameters in the field.

There are few publications addressing the subcritical flow regime through wellhead chokes, examples of these papers include Fortunati [32], Ashford and Pierce [14], Pilehvari [31], Sachdeva et al. [2], Surbey et al. [33], Elgibaly and Nashawi [25], Al-Attar [34], AlAjmi et al. [35], Nasriani and Kalantariasl [36] and Seidi and Sayahi [3]. Al-Attar [34] used a plotting technique to describe the subcritical flow behavior of gas condensate in three wells located in the Middle East. They found that this approach is superior to the application of a nonlinear regression analysis on a modified version

of the Gilbert-type formula (replace  $P_u$  by  $\Delta P$  in Gilbert model [9]). Nasriani and Kalantariasl [36] extended the plotting technique of Al-Attar [34] and his modified Gilbert-type formula to describe the subcritical flow of high rate gas condensate wells with large choke sizes located in Iran.

Petroleum engineers have shown a high degree of open-mindedness in utilizing new technologies from different disciplines to solve old and new petroleum engineering problems. Ghorbani et al. [37] used a nonlinear and evolutionary optimization algorithms of an Excel solver and a genetic algorithm to calculate the coefficients of a modified Gilbert model in which they added basic sediment and water parameter. They used a data set of 182 measurements of the Reshadat offshore oil field of Iran to find the coefficients that best fit these data. They found that the models obtained by the two algorithms of the Excel solver outperform the other models including their model of the genetic algorithm, Gilbert [9], Baxendell [30], Ros [11], Achong [24], Safar Beiranvand et al. [38] and Mirzaei-Paiaman and Salavati [29] models. Choubineh et al. [8] used an artificial neural network algorithm combined with teaching-learning-based optimization algorithm to predict the liquid flow rate in the critical regime. They introduced three parameters to the Gilbert model: gas specific gravity, oil specific gravity and temperature. They conducted an experimental study on a data set of 113 well-head flow tests from the oil wells in south Iran, and they compared the accuracy of their models with some published models in the literature. Seidi and Sayahi [3] established, for the subcritical two-phase flow regime, a new Gilbert-type correlation on the basis of Nasriani and Kalantariasl [36] correlation by adding to the pressure drop an exponent. They used a genetic algorithm and a nonlinear regression technique. The new models as well as other models from the literature have been tested on 67 measurements of 10 different fields in high rate gas condensate reservoirs in south Iran and on 39 data points gathered from gas condensate wells of Fars province of Iran. They found that the nonlinear regression analysis is more efficient in fitting the data in comparison with the genetic algorithm. AlAjmi et al. [35] used an artificial neural network algorithm to predict the oil flow rate for the critical and subcritical regimes. They added the temperature and water cut to the parameters of the Gilbert model. In the case of the subcritical regime, the downstream pressure is included in the model together with the latter two parameters. Mirzaei-Paiaman and Salavati [39] also used an artificial neural network technique to predict the oil flow rate in two-phase flow through wellhead chokes using upstream pressure, choke size and producing gas to oil ratio. The accuracy of the developed model was compared to the Gilbert [9], Baxendell [30], Achong [24] and Mirzaei-Paiaman and Salavati [29] models.

### 3 Models Expressions and Methodology

On the above methods, only few approaches can be applied for the subcritical regime and significant errors may result from the application of the current correlations to predict choke performance under multiphase flow conditions of the HMD field wells. For this reason, the aim of this study is to develop simple, yet accurate, models for estimating the oil flow rate under critical and subcritical flow conditions through chokes of naturally flowing wells and of wells that are assisted with gas lift in the HMD oil field. The model that is used actually in the HMD field is a function of the choke size, the flowline pressure, the wellhead pressure and an adjustable parameter. Correlations were used to find out the constants and the variable exponents of this model that best fit the measured data.

Most of the studies published in the literature to compare the existing models reveal the accuracy of the correlations derived from the Gilbert model [9]. This model possesses also the practical advantages of having few variables that are available in most of the fields (by telemetry or in the data bank) as compared with other approaches that require many parameters (e.g., the PVT properties of the produced fluids). However, the Gilbert model is valid only under the critical flow conditions in which the flow rate reaches a maximum value that is independent of the pressure drop across the choke, but in the subcritical regime, changes in the pressure downstream the choke affects the flow rate. Al-Attar [34] and Nasriani and Kalantariasl [36] substituted pressure drop for upstream pressure in Gilbert formula to predict the choke performance under subcritical flow conditions of gas condensates. Seidi and Sayahi [3] added an exponent to the pressure drop to consider the fact that the relation between the pressure and the flow passing through the chokes of gas condensate wells is not always a straight line but may be concave to the origin.

Elgibaly and Nashawi [25] proposed another extension of the Gilbert model [9] for the subcritical regime. This extension is given in Eq. (2). They justify the form of their model by the fact that the relationship between the pressure drop across the choke and the flow rate is quadratic and plots as a parabola.

$$Q = \left[ a \frac{\Delta P \cdot \phi^b}{GLR^c} \right]^{(1/2)} \quad (2)$$

In this study, two new forms of the Gilbert model are proposed and tested on the data of 178 wells of the HMD field. These models are valid for both critical and subcritical regimes. In the first model, the flowline pressure ( $P_d$ ) is introduced in a ratio with an exponent. Since the threshold of



the critical flow in HMD is taken 0.75, the developed model is given as follows:

$$Q = a \frac{P_u \cdot \phi^b}{GOR^c} \cdot f(P_u, P_d), \quad \text{where}$$

$$f(P_u, P_d) = \begin{cases} 1, & \text{if } \frac{P_d}{P_u} \leq 0.75 \text{ (critical flow)} \\ [f_1(P_d, P_u)]^d, & \text{otherwise (subcritical flow).} \end{cases} \quad (3)$$

where GOR (MSCF/BBL).

The second model is obtained by introducing a function that is used in the equation applied currently in HMD field for the subcritical regime without an exponent, the resulting model is:

$$Q = a \frac{P_u \cdot \phi^b}{GOR^c} \cdot f(P_u, P_d), \quad \text{where}$$

$$f(P_u, P_d) = \begin{cases} 1, & \text{if } \frac{P_d}{P_u} \leq 0.75 \text{ (critical flow)} \\ f_2(P_d, P_u), & \text{otherwise (subcritical flow).} \end{cases} \quad (4)$$

$f_1$  and  $f_2$  are functions of  $P_d$  and  $P_u$  (see Sect. 4).

The nonlinear regression algorithm of Levenberg–Marquardt [40,41] was applied to determine the values of the constants and the variables exponents of the models that best fit the measured data. Nonlinear regression is based on an iterative process which is able to fit the measured data with a parameterized function that nonlinearly depends on one or more parameters. This approach is often used when there are physical reasons for believing that the data and the parameters follow a particular functional form [42]. The parameters are estimated by minimizing the sum of the squares of the differences between the data points and the function, but other criteria can be considered as well if it is desired to protect against non-normal errors.

Among the existing algorithms, Levenberg–Marquardt is a popular method to solve nonlinear least squares problems effectively due to its ability to converge from a wide range of initial solutions [43]. This algorithm interpolates between the gradient descent method and the Gauss–Newton method. In the gradient descent method, the sum of the squared errors is reduced by updating the parameters in the steepest-descent direction. In the Gauss–Newton method, the sum of the squared errors is reduced by assuming that the least squares function is locally quadratic and finding the minimum of the quadratic. When the solution is far from the minimum, the Levenberg–Marquardt algorithm behaves more like a gradient-descent method. However, as the solution gets closer to the minimum, it acts more like the Gauss–Newton method.

Given a set of  $m$  data measurements  $(x_i, y_i)$  and a function  $f$  of a vector parameter  $\theta$  and a vector variable  $x$ , the objective is to minimize the sum of the squares of the errors:

$$E(\theta) = \sum_{i=1}^m [y_i - f(x_i; \theta)]^2 \quad (5)$$

The basis of the algorithm is a linear approximation of  $f$  in the neighborhood of  $\theta$ . For a small  $\|\delta_\theta\|$ , a Taylor series expansion leads to the approximation

$$f(x_i; \theta + \delta_\theta) \approx f(x_i; \theta) + \mathbf{J}_i \delta_\theta \quad (6)$$

where  $\mathbf{J}_i = \frac{\partial f(x_i; \theta)}{\partial \theta}$ . From an initial point  $\theta_0$ , the algorithm produces a series of vectors  $\theta_1, \theta_2, \dots$  that converge toward a minimum for  $E$ . Hence, at each step, it is required to find the  $\delta_\theta$  that minimizes  $E(\theta + \delta_\theta)$ . This leads to:

$$(\mathbf{J}^T \mathbf{J}) \delta_\theta = \mathbf{J}^T [Y - F(\theta)] \quad (7)$$

where  $\mathbf{J}$  is the Jacobian matrix, whose  $i$ -th row equals  $\mathbf{J}_i$ , and where  $F(\theta)$  and  $Y$  are vectors with  $i$ -th component  $f(x_i; \theta)$  and  $y_i$ , respectively. Levenberg [40] proposed the following search scheme to update the parameter:

$$(\mathbf{J}^T \mathbf{J} + \lambda I) \delta_\theta = \mathbf{J}^T [Y - F(\theta)] \quad (8)$$

where  $I$  is the identity matrix and  $\lambda$  is a damping factor. Small values of  $\lambda$  result in a Gauss–Newton update and large values of  $\lambda$  result in a gradient descent update. Marquardt [41] suggested to replace  $I$  with the diagonal of  $\mathbf{J}^T \mathbf{J}$  resulting into the Levenberg–Marquardt algorithm:

$$(\mathbf{J}^T \mathbf{J} + \lambda \text{diag}(\mathbf{J}^T \mathbf{J})) \delta_\theta = \mathbf{J}^T [Y - F(\theta)] \quad (9)$$

### 4 Models Evaluation

For the purpose of this study, a large set of critical and sub-critical production tests consisting of choke size, wellhead and flowline pressures, gas–oil ratio and oil flow rate were collected from three satellites of the HMD oil field. A satellite refers to a set of wells that are related to the same separator. The production tests were taken from portable separators designed for well testing. The set of data is divided into three sets corresponding to the three satellites. The first (second and third respectively) set contains 1,255 (1,025 and 4,506, respectively) data points that considers all the history of 41 (41 and 92, respectively) wells of the first (second and third, respectively) satellite. The broad ranges covered by the various flow parameters of these data are listed in Table 2. The number of data points of each flow regime and of each range of GOR is given in Tables 6, 7, 8, 9, 10, 11, 12, 13, and 14 for the first satellite.

For each set of data, a comparison between the Gilbert model [9] and the model that is used actually in the HMD

**Table 2** Different parameter ranges of the data tests

| Parameters  | $\phi$ (1/64 in.) |        | $Q$ (bbl/day) |         | GOR (MSCF/BBL) |         | $P_u$ (psia) |         | $P_d$ (psia) |         |
|-------------|-------------------|--------|---------------|---------|----------------|---------|--------------|---------|--------------|---------|
|             | min               | max    | min           | max     | min            | max     | min          | max     | min          | max     |
| Satellite 1 | 17.64             | 129.99 | 1.51          | 4077.43 | 0.084          | 1273.18 | 120.87       | 2149.50 | 28.44        | 487.75  |
| Satellite 2 | 22.68             | 107.09 | 1.51          | 7754.82 | 0.129          | 1022.87 | 119.45       | 1399.25 | 32.00        | 543.20  |
| Satellite 3 | 15.12             | 94.01  | 21.13         | 3938.55 | 0.112          | 92.12   | 126.558      | 3697.2  | 29.862       | 679.716 |

field (called in what follows the current model) is first performed. Then, in order to correlate the parameters of Eqs. (1), (3) and (4), the data points of each set are divided for each flow regime into five subsets representing five GOR intervals (the unit  $\text{sm}^3/\text{m}^3$ ):  $0 \leq \text{GOR} < 250$ ,  $250 \leq \text{GOR} < 550$ ,  $550 \leq \text{GOR} < 750$ ,  $750 \leq \text{GOR} < 1000$  and  $\text{GOR} \geq 1000$ . A global comparison including these models along with the Gilbert [9] and Elgibaly and Nashawi [25] models is conducted, and the best models are selected to examine their applicability in comparison to the current one. The performance criteria used to estimate the accuracy of the different models are:

$$\text{SAD} = \sum |Q_e - Q_m| \quad (10)$$

$$\text{SD} = \sum (Q_e - Q_m) \quad (11)$$

$$\text{RAE} = \frac{|Q_e - Q_m|}{Q_m} \quad (12)$$

$$\text{RE} = \frac{Q_e - Q_m}{Q_m} \quad (13)$$

We also calculated the minimum, mean and maximum of the relative absolute error in percentage (MinRAE, MeanRAE and MaxRAE, respectively) and the minimum, mean and maximum of the relative error in percentage (MinRE, MeanRE and MaxRE, respectively). The results of the first satellite are summarized in the Appendix in Tables 6, 7, 8, 9, 10, 11, 12, 13, and 14.

#### 4.1 Study A

In this study, the current model and the correlation proposed by Gilbert [9] (by replacing GLR with GOR) are tested against the measured data of the three satellites. The results are depicted in Figs. 1, 2, 3, 4 and 5. Table 3 summarizes the SAD of the two models and the percentage of improvement (IMP) in comparison to the current model, note that  $\nearrow$  indicates an increase in the SAD.

Figure 1 presents the mean of SAD of the two models on all the wells of the first satellite corresponding to the first set of data. The results show that the Gilbert model performs better than the current model in 34 wells out of 41, and the SAD was reduced by 17.40% (from  $1678.36 \text{ m}^3/\text{h}$  to  $1386.27 \text{ m}^3/\text{h}$  on 1,255 measurements). Regarding the second (respectively,

the third) satellite corresponding to the second (respectively, third) set of data, the Gilbert model outperforms the current model in 24 wells out of 41 (respectively, in 40 wells out of 92) and the SAD decreased by 8.48% on 1,025 measurements (respectively increased by 9.93% on 4,506 measurements).

Note that the Gilbert model considers the gas–oil ratio which is not included in the current model. In contrast, this latter takes into account the downstream pressure of the choke under the subcritical flow conditions that does not appear in the Gilbert model. To study the impact of these two parameters, further analysis has been performed: A comparison between the results of the two models on the wells that are assisted with gas lift (known with high GOR values) and on the naturally flowing wells, and a comparison between the two models on the two flow regimes for different GOR intervals.

Figure 2 shows the results obtained on the wells when they were assisted with gas lift. Clearly, the Gilbert model is more efficient than the current model in 32 wells out of 35, and the SAD was reduced by 27.62% (from  $1292.05$  to  $935.20 \text{ m}^3/\text{h}$  on 933 measurements). However, by considering the measurements in which the wells were naturally flowing (see Fig. 3), improvements have been observed in only 9 wells out of 33 and the SAD increased by 14.36% (from  $386.31$  to  $451.08 \text{ m}^3/\text{h}$  on 322 measurements). Regarding the second (respectively, the third) satellite, the Gilbert model was more efficient in 19 wells out of 25 (respectively, 27 wells out of 33) by considering the measurements in which the wells were assisted with gas lift and the SAD was reduced by 24.31% on 684 measurements (respectively, by 19.48% on 700 measurements). When the wells were naturally flowing, the Gilbert model was less efficient, improvements have been obtained in 14 wells out of 34 (respectively in 30 out of 92) and the SAD increased by 19.45% on 341 measurements (respectively, 15.41% on 3806 measurements).

It can be concluded from these results that the accuracy of the oil flow rate estimation clearly depends on the gas–oil ratio. The Gilbert model yields better results on the wells that are assisted with gas lift even if the downstream pressure of the choke is not considered. However, the current model is more efficient on the naturally flowing wells that are known with low GOR values. This latter observation can

**Fig. 1** First satellite: comparison between the current and the Gilbert models by wells

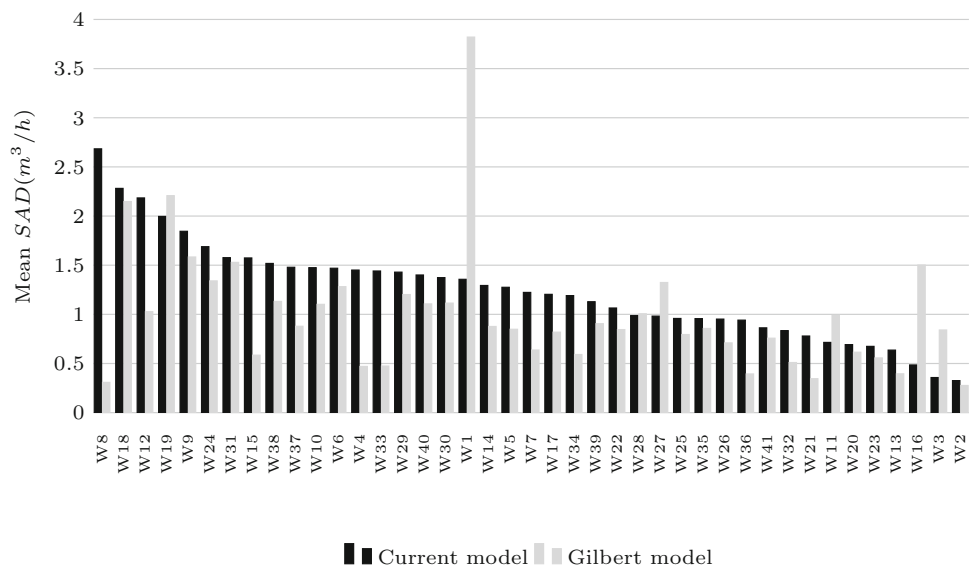


**Fig. 2** First satellite: comparison between the current and the Gilbert models when the wells were assisted with Gas Lift

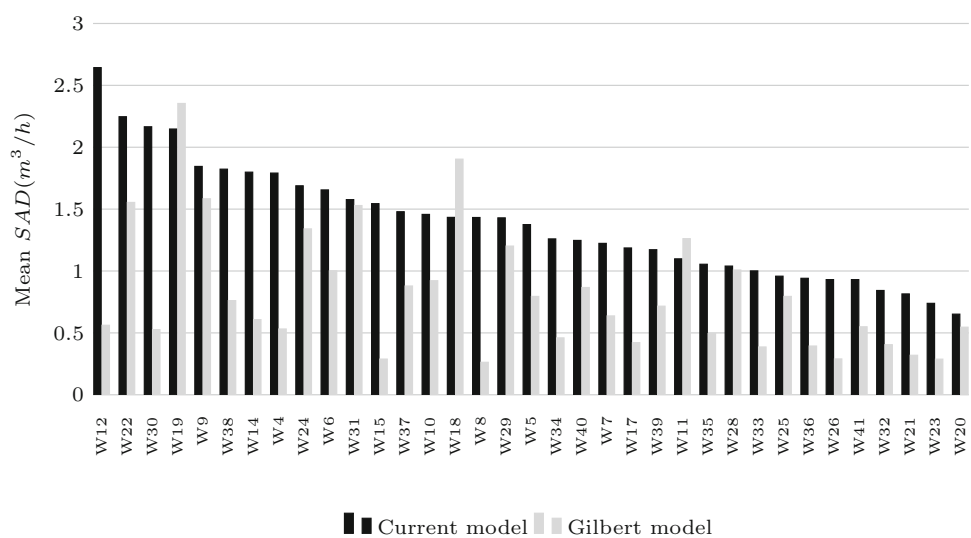


**Fig. 3** First satellite: comparison between the current and the Gilbert models when the wells were naturally flowing

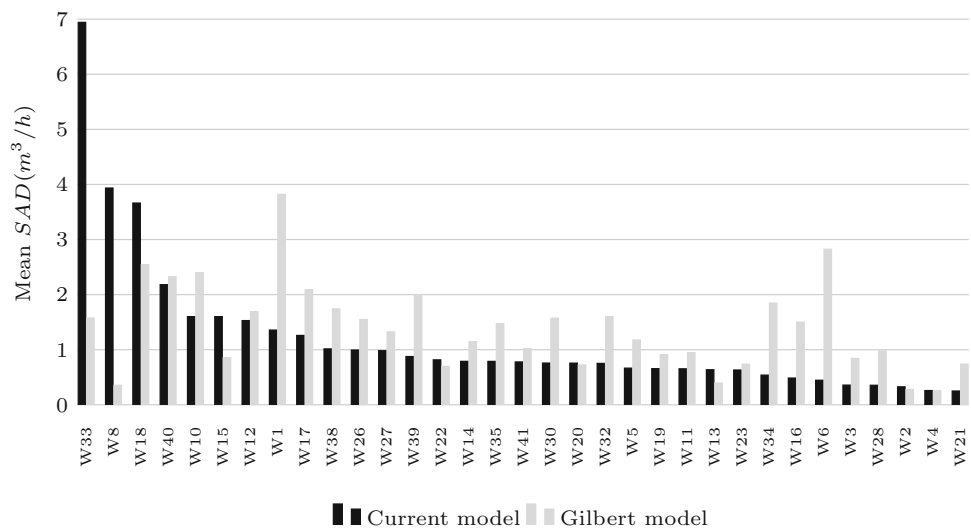


**Fig. 4** First satellite: comparison between the current and the Gilbert models under critical regime for different GOR intervals

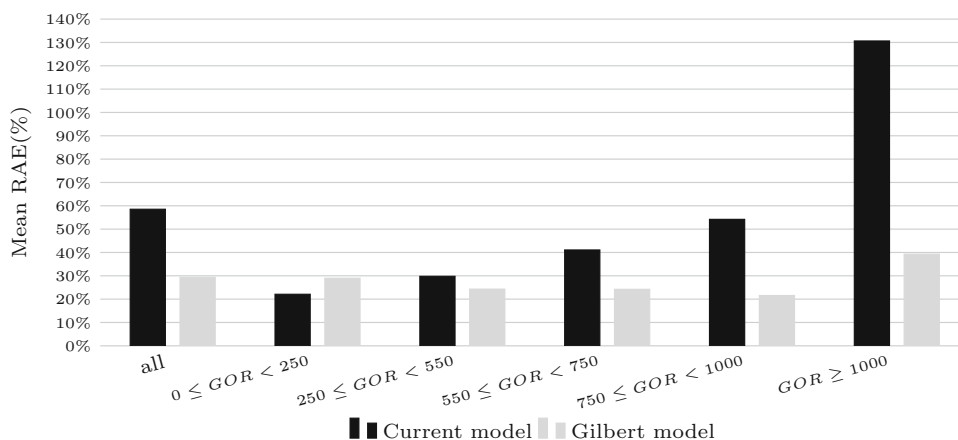


**Fig. 5** First satellite: comparison between the current and the Gilbert models under subcritical regime for different GOR intervals

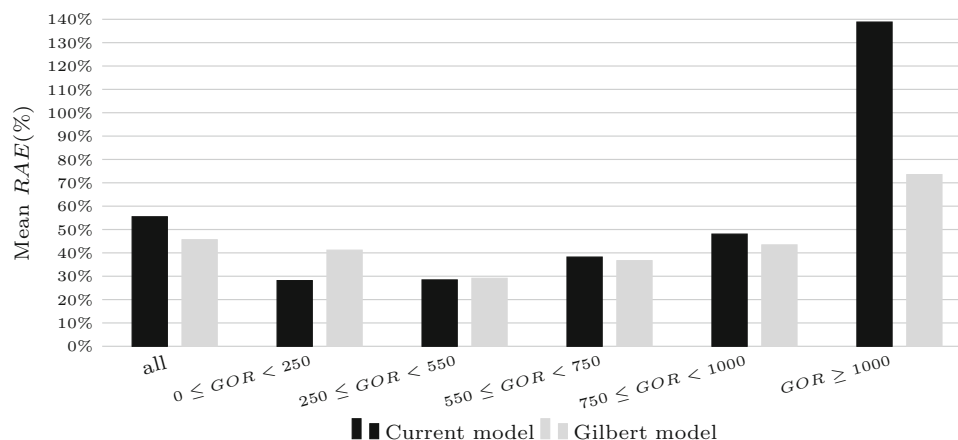


**Table 3** SAD (m<sup>3</sup>/h) of the Gilbert [9] model on each satellite in comparison to the current model

| Wells' status | Satellite 1 |          |                   | Satellite 2 |          |                   | Satellite 3 |          |                   |
|---------------|-------------|----------|-------------------|-------------|----------|-------------------|-------------|----------|-------------------|
|               | All         | Gas lift | Naturally flowing | All         | Gas lift | Naturally flowing | All         | Gas lift | Naturally flowing |
| Current model | 1678.36     | 1292.05  | 386.31            | 1422.97     | 908.19   | 514.78            | 6038.02     | 948.31   | 5089.71           |
| Gilbert model | 1386.27     | 935.20   | 451.08            | 1302.34     | 687.43   | 614.91            | 6637.54     | 763.55   | 5873.99           |
| IMP (%)       | 17.40       | 27.62    | 14.36 ↗           | 8.48        | 24.31    | 19.45 ↗           | 9.93 ↗      | 19.48    | 15.41 ↗           |

be explained by the fact that the current model introduces the downstream pressure of the choke in the subcritical regime.

Figures 4 and 5 present the mean of the RAE in percentage of both models for different GOR intervals (the unit is sm<sup>3</sup>/m<sup>3</sup>) under critical and subcritical regimes, respectively, of the first satellite. As it can be observed, the performance of the current model decreases while increasing the GOR and this is under both flow regimes, whereas the Gilbert model has a more stable performance and performs better under the critical regime. Furthermore, the current model provides the best accuracy with the least mean RAE for low GOR values (0 ≤ GOR < 250 for the critical regime and 0 ≤ GOR < 550 for the subcritical regime). However, the Gilbert model does quite better for high values of GOR. On the other two satellites, we obtained the same conclusions.

These results reveal again the impact of the GOR on the oil flow rate. For low GOR values and under the subcritical regime, the effect of the downstream pressure of the choke can be observed since the efficiency of the current model increases in comparison to the Gilbert model. On the other hand, one can observe that the error between the measured and the estimated flow rate obtained by the two models is important especially for high GOR values; this led us to develop new models that best fit the data of the field all by taking into account the impact of the GOR and the downstream pressure of the choke.



**Fig. 6** First satellite: comparison between the Gilbert and the revised Gilbert models under the critical regime for different GOR intervals

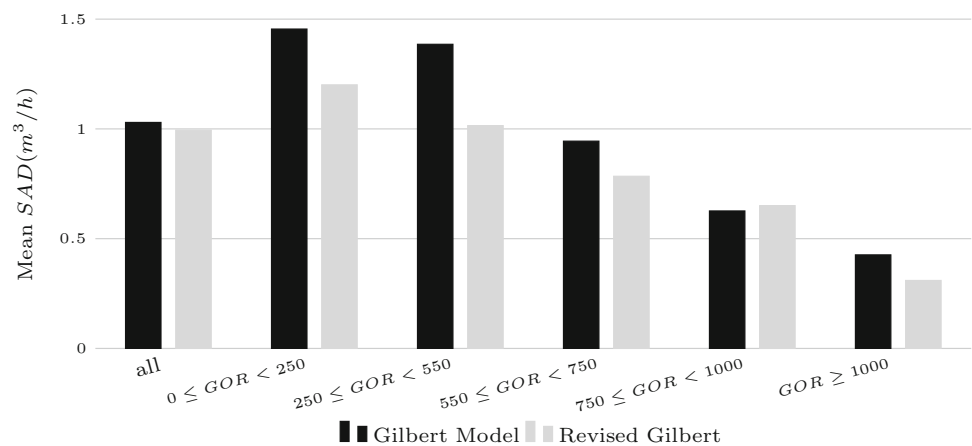
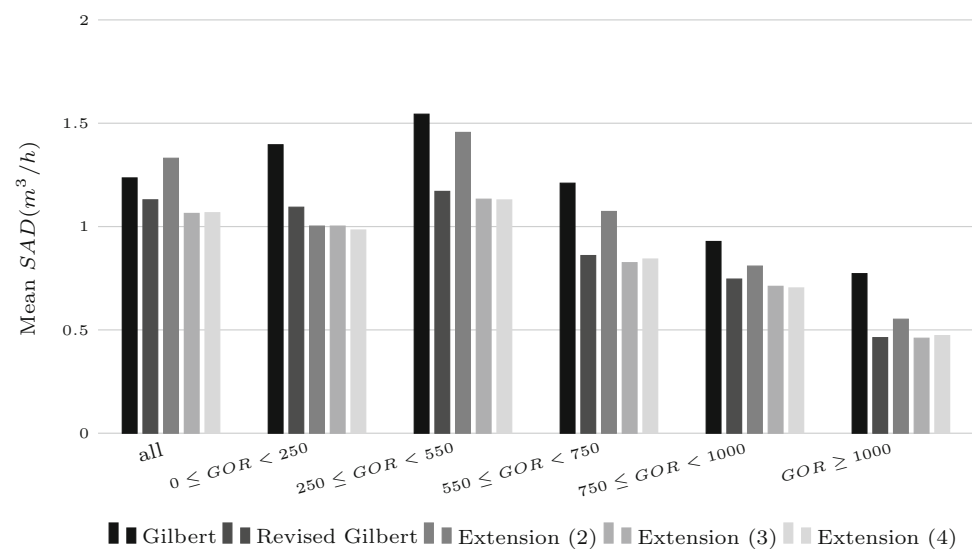


**Fig. 7** First satellite: comparison between the Gilbert model and its variants under the subcritical regime for different GOR intervals



**4.2 Study B**

In this study, the models given in Eqs. (1), (2), (3) and (4) are evaluated and validated. The constants and the variable exponents were calculated using the nonlinear regression algorithm of Levenberg–Marquardt [40,41] to find out the correlations that best fit the measured data. As observed in the previous section, the GOR has a major effect on the accuracy of the oil flow rate estimation; for this reason, we applied the Levenberg–Marquardt algorithm on different GOR intervals, and this is for both critical and subcritical regimes to achieve a better accuracy. In Eqs. (1) and (2), the GOR is used rather than the GLR. The results are depicted in Figs. 6 and 7 and summarized in Table 4. Note that, in Table 4, IMP is calculated for the best extension in comparison to the Gilbert model [9], and the bold values indicate the best SAD for each satellite.

Under the critical flow conditions, Eqs. (1), (2), (3) and (4) have the same form and the results of the correlation obtained by applying the Levenberg–Marquardt algorithm

(denoted revised Gilbert) on the first satellite are given in Fig. 6 and Table 4 along with the results of the Gilbert correlation [9]. Figure 6 shows that the revised Gilbert correlation yielded better results in general. In addition, the SAD was reduced by 20.79% (from 820.48 to 649.92 m³/h on 797 measurements) when using the curve-fitting technique on the five GOR ranges rather than 3.41% (from 820.48 to 792.56 m³/h) obtained by applying the curve-fitting on all the measurements of the critical regime.

Regarding the second and the third satellites (see Table 4), the revised Gilbert correlation outperforms the Gilbert correlation on all the GOR intervals. When using the curve-fitting technique on the five GOR ranges, the SAD of the second satellite (respectively, the third satellite) was reduced by 20.12% (respectively, by 10.77%), from 608.23 to 485.87 m³/h on 620 measurements (respectively, from 5319.35 to 4746.60 m³/h on 3482 measurements), and by 3.05% (respectively, by 3.60%), from 608.23 to 589.65 m³/h (respectively, from 5319.35 to 5127.70 m³/h), when applying the curve-fitting on all the measurements of the critical

**Table 4** SAD (m<sup>3</sup>/h) of the different extensions in comparison with the Gilbert model [9] for the critical and the subcritical regimes

| Models          | Satellite 1   | Satellite 2   | Satellite 3    |
|-----------------|---------------|---------------|----------------|
| Critical        |               |               |                |
| Gilbert         | 820.48        | 608.23        | 5319.35        |
| Revised Gilbert | <b>649.92</b> | <b>485.87</b> | <b>4746.60</b> |
| IMP(%)          | 20.79         | 20.12         | 10.77          |
| Subcritical     |               |               |                |
| Gilbert         | 565.79        | 694.11        | 1318.18        |
| Revised Gilbert | 421.20        | 471.18        | 947.21         |
| Extension (2)   | 544.4         | 670.19        | 1056.28        |
| Extension (3)   | 397.97        | <b>455.09</b> | 888.26         |
| Extension (4)   | <b>396.13</b> | 465.31        | <b>881.24</b>  |
| IMP (%)         | 29.98         | 34.43         | 33.15          |

regime. Therefore, fitting the data on different GOR intervals minimizes the error between the measured and the estimated rate and improves the ability of the model to predict the oil flow rate.

Figure 7 summarizes the results obtained on the first satellite in the subcritical regime. Extensions (2), (3) and (4) denote the models of Eqs. (2), (3) and (4), respectively. Recall that in extension (3) the  $P_d$  is introduced in a ratio ( $f_1(P_d, P_u) = \frac{P_d}{P_u}$ ) and the coefficient  $d$  in extension (4) equals  $-1.2$  ( $f_2(P_d, P_u) = [f_1(P_d, P_u)]^{-1.2}$ ). As it can be observed, extensions (3) and (4) seem to be the most efficient followed by the revised Gilbert model, whereas extension (2) and the Gilbert model were not satisfactory. Furthermore, extensions (3) and (4) are closely competitive; however, extension (4) yielded better results in overall (see Table 4). On the other hand, the SAD of the Gilbert model was reduced by 29.98% (from 565.79 to 396.13 m<sup>3</sup>/h on 458 measurements) when using the curve-fitting technique for extension (4) on the five GOR intervals rather than 13.63% obtained by applying the curve-fitting on all the measurements of the subcritical regime.

The observations obtained on the accuracy of the five models on the other two satellites were the same in comparison with the first satellite (see Table 4). However, on the second satellite, the model of extension (3) seems to be more efficient in overall than extension (4). The SAD of the Gilbert model on the second satellite (respectively, third satellite) was reduced by 34.43% (respectively, by 33.15%), from 694.11 to 455.09 m<sup>3</sup>/h on 405 measurements (respectively, from 1318.18 to 881.24 m<sup>3</sup>/h on 1,024 measurements), when using the curve-fitting technique of extension (3) (respectively, of extension (4)) on the five GOR intervals. Again, the ability of the models to estimate the flow rate is found to be improved when applying the Levenberg–Marquardt algorithm on different GOR ranges.

The comparison between the revised Gilbert model and extensions (3) and (4) shows the characteristics of the subcritical flow of the production tests used in this study. Adding the downstream pressure of the choke in the model was essential to improve the accuracy of the models, since under the subcritical regime any downstream disturbance is able to influence the upstream conditions and changes in the downstream pressure of the choke affect the flow rate. The results also show that extensions (3) and (4) are closely comparable; this can be explained by the fact that the exponent  $d$  obtained in extension (3) (see Table 13) is close to the coefficient used in extension (4). It is worth noting that the accuracy of the new models increases while increasing the GOR values.

### 4.3 Global Comparison

Now, a comparison between the current model used in HMD field and the best model derived from study B is performed (see Figs. 8, 9, 10 and Table 5). In the first satellite, improvements have been observed in 39 wells out of 41 by applying extension (4) (see Fig. 8) and the SAD was reduced by 37.67%. By considering the measurements in which the wells were assisted with gas lift, the prediction of the oil flow rate was improved in all the wells (see Fig. 9) and the SAD was reduced by 42.80% (from 1292.05 to 739.08 m<sup>3</sup>/h on 933 measurements). However, when the wells were naturally flowing, improvements have been obtained on 21 wells out of 33 (see Fig. 10) and the SAD was reduced by 20.54% (from 386.31 to 306.97 m<sup>3</sup>/h on 322 measurements).

For the second (respectively, third) satellite (see Table 5), the prediction of the oil flow rate was improved in 33 wells out of 41 (respectively, 58 wells out of 92) and the SAD was reduced by 33.87% on 1,025 measurements (respectively, by 6.79% on 4,506 measurements). For the measurements in which the wells were assisted with gas lift, improvements have been obtained in 22 wells out of 25 (respectively,

**Fig. 8** First satellite: comparison between the current model and extension (4) by wells

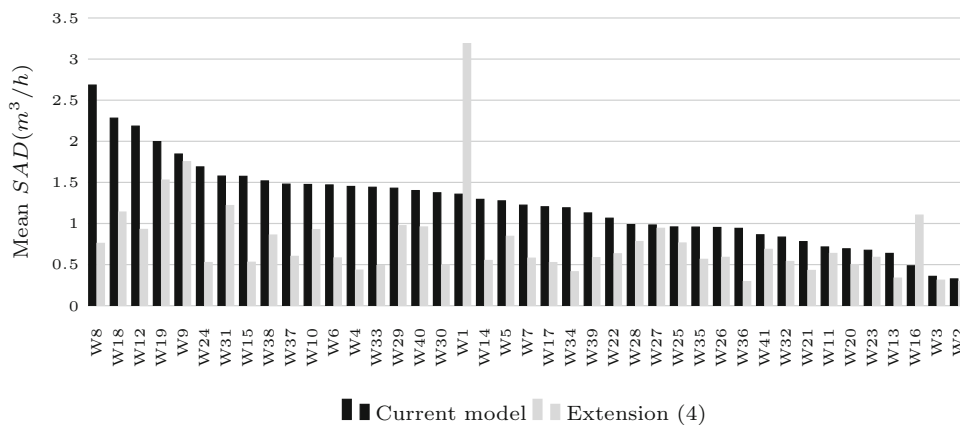


**Fig. 9** First satellite: comparison between the current model and extension (4) by wells when they were assisted with gas lift

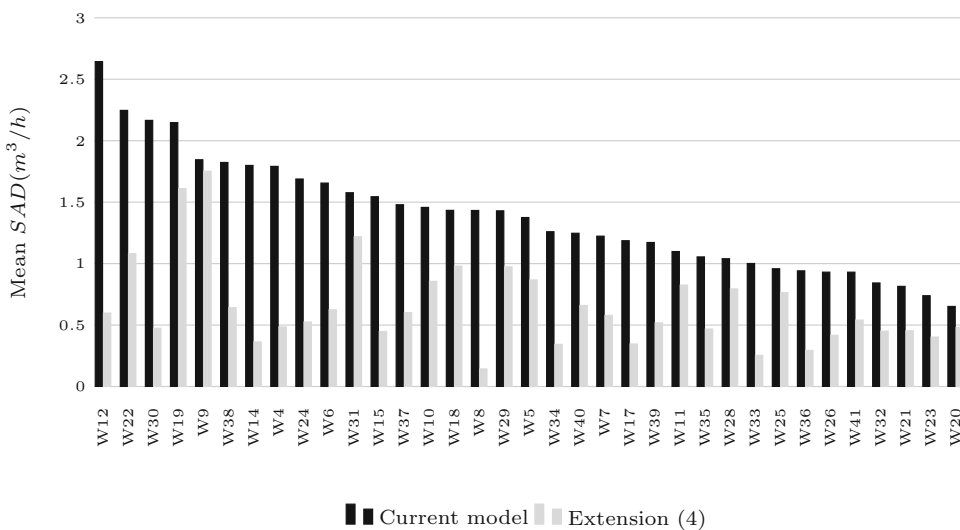


**Fig. 10** First satellite: comparison between the current model and extension (4) by wells when the wells were naturally flowing

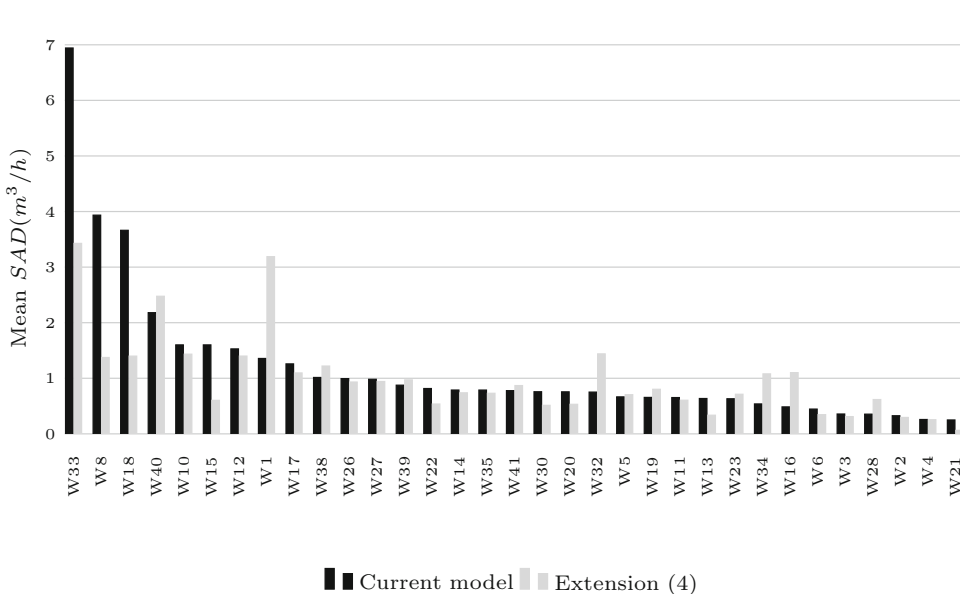


**Table 5** SAD (m<sup>3</sup>/h) of the Gilbert [9] model and the best extension on each satellite in comparison to the current model

| Wells' status  | Satellite 1 |          |                   | Satellite 2 |          |                   | Satellite 3 |          |                   |
|----------------|-------------|----------|-------------------|-------------|----------|-------------------|-------------|----------|-------------------|
|                | All         | Gas lift | Naturally flowing | All         | Gas lift | Naturally flowing | All         | Gas lift | Naturally flowing |
| Current model  | 1678.36     | 1292.05  | 386.31            | 1422.97     | 908.19   | 514.78            | 6038.02     | 948.31   | 5089.71           |
| Best extension | 1046.05     | 739.08   | 306.97            | 940.96      | 512.60   | 428.36            | 5627.84     | 571.05   | 5056.79           |
| IMP (%)        | 37.67       | 42.80    | 20.54             | 33.87       | 43.56    | 16.79             | 6.79        | 39.78    | 0.65              |

28 wells out of 33) and the SAD was reduced by 43.56% (respectively, by 39.78%), from 908.19 to 512.60 m<sup>3</sup>/h on 684 measurements (respectively, from 948.31 to 571.05 m<sup>3</sup>/h on 700 measurements). However, when the wells were naturally flowing, the prediction was improved in 20 wells out of 34 (respectively, in 50 wells out of 92), and the SAD was reduced by 16.79% (respectively, by 0.65%), from 514.78 to 428.36 m<sup>3</sup>/h on 341 measurements (from 5089.71 to 5056.79 m<sup>3</sup>/h on 3,806 measurements).

Based on these results, the estimated flow rate with the new models show a clear superiority to the estimated rate obtained by the current model. The comparison between the results obtained in study A and this section confirms the fact that incorporating the upstream pressure of the choke in the subcritical regime and fitting the data on different GOR intervals improve the accuracy of the oil flow rate estimation considerably.

## 5 Conclusion

New multiphase flow models for the prediction of the oil flow rate through wellhead chokes of naturally flowing wells and of wells that are assisted with gas lift are developed and evaluated under critical and subcritical flow conditions. These models were derived from the Gilbert model which is known, besides its accuracy, by the fact that it is simple to use in practice since the parameters required are routinely measured in the field. The validity of the proposed models along with three existing models was tested on a data set of 6,786 measurements containing the history of 174 wells of three satellites located in the HMD oil field.

Statistical error analysis showed that the two new models [extensions (3) and (4)] delivered the best accuracy (in comparison with the Gilbert correlation [9] and the Elgibaly and Nashawi [25] model of Eq. 2) especially for the wells that are assisted with gas lift. In the latter case, the two extensions yielded better results than the current model in 85 wells out of 93 and the SAD was reduced by 42.11% on 2,317 measurements. On the wells that are naturally flowing, the efficiency of the two extensions decreases but they are still more efficient than the other models, and we had improvements, in comparison with the current model, in 91 wells out of 159

and the SAD was reduced by 3.32% on 4,469 measurements. In overall, the two extensions outperform the current model in 130 wells out of 174 and the SAD was reduced by 16.68% on 6,786 measurements.

Incorporating the downstream pressure of the choke in the new models [extensions (3) and (4)] to handle the subcritical conditions improved the predictive accuracy. Furthermore, the precision of these models has been found to be significantly improved when applied to different GOR ranges. For this reason, the nonlinear multivariable regression of Levenberg–Marquardt algorithm has been applied to five GOR intervals on each flow regime to find out the correlations that best fit the measured data. Among the wide ranges of the gas–oil ratio used in this investigation, the new models yielded the minimum error for high GOR values ( $GOR \geq 550 \text{ sm}^3/\text{m}^3$ ).

The proposed models are applicable for a wide range of input variables covered by the data set of this study and on conditions similar to those of the HMD oil field.

More tests should be conducted on the other satellites (oil, gas, and gas condensate wells) of the HMD field and on other fields especially with data representing subcritical flow in order to benchmark the accuracy of the models further. From the work performed on HMD, it is recommended to calibrate the coefficients of the models on different GOR ranges and by separating the naturally flowing wells and the wells that are assisted with gas lift. It is also important to correlate data collected from wells that have similar PVT characteristics in order to better fit the measurements.

**Acknowledgements** The authors gratefully wish to thank Farid CHEMIL, Aissa DAHMOUNE and Boutheyna FARTAS (Production Division, Sonatrach, Hassi-Messaoud) for their support to achieve this work.

## Appendix

In this section, we present the results we obtained on the first satellite by the six models (Tables 6, 7, 8, 9, 10, 11, 12, 13, 14).

**Table 6** First satellite: results of the current model under the critical regime

| Constraint       | Nb data | MinRAE (%) | MeanRAE (%) | MaxRAE (%) | MinRE (%) | MeanRE (%) | MaxRE (%) | SAD (m <sup>3</sup> /h) | SD (m <sup>3</sup> /h) |
|------------------|---------|------------|-------------|------------|-----------|------------|-----------|-------------------------|------------------------|
| All              | 797     | 0.00       | 58.52       | 6503.14    | -97.67    | 36.01      | 6503.14   | 1088.08                 | 334.58                 |
| 0 ≤ GOR < 250    | 210     | 0.00       | 22.09       | 207.36     | -97.67    | -0.65      | 207.36    | 245.85                  | -26.57                 |
| 250 ≤ GOR < 550  | 214     | 0.014      | 29.78       | 354.14     | -79.83    | 9.24       | 354.14    | 332.88                  | 80.24                  |
| 550 ≤ GOR < 750  | 89      | 0.24       | 41.07       | 550.24     | -85.64    | 14.74      | 550.24    | 124.52                  | 33.42                  |
| 750 ≤ GOR < 1000 | 67      | 1.83       | 54.19       | 475.85     | -93.05    | 27.46      | 475.85    | 111.09                  | 54.85                  |
| GOR ≥ 1000       | 217     | 0.50       | 130.63      | 6503.14    | -85.26    | 109.27     | 6503.14   | 273.73                  | 192.64                 |

**Table 7** First satellite: results of the current model under the subcritical regime

| Constraint       | Nb data | MinRAE (%) | MeanRAE (%) | MaxRAE (%) | MinRE (%) | MeanRE (%) | MaxRE (%) | SAD (m <sup>3</sup> /h) | SD (m <sup>3</sup> /h) |
|------------------|---------|------------|-------------|------------|-----------|------------|-----------|-------------------------|------------------------|
| All              | 458     | 0.03       | 55.46       | 2326.93    | -0.03     | 26.58      | 2326.93   | 590.28                  | 70.92                  |
| 0 ≤ GOR < 250    | 182     | 0.03       | 28.12       | 204.98     | -0.03     | 1.07       | 204.98    | 208.26                  | -28.13                 |
| 250 ≤ GOR < 550  | 94      | 0.29       | 28.42       | 219.81     | -84.91    | -5.97      | 219.81    | 123.37                  | -28.82                 |
| 550 ≤ GOR < 750  | 49      | 0.91       | 38.20       | 220.40     | -77.80    | 4.83       | 220.40    | 60.21                   | 0.70                   |
| 750 ≤ GOR < 1000 | 30      | 5.36       | 48.04       | 157.42     | -91.92    | 1.43       | 157.42    | 34.19                   | -4.923637              |
| GOR ≥ 1000       | 103     | 0.28       | 138.82      | 2326.93    | -96.39    | 119.03     | 2326.93   | 164.25                  | 132.09                 |

**Table 8** First satellite: results of the Gilbert correlation under the critical regime

| Constraint       | Nb data | MinRAE (%) | MeanRAE (%) | MaxRAE (%) | MinRE (%) | MeanRE (%) | MaxRE (%) | SAD (m <sup>3</sup> /h) | SD (m <sup>3</sup> /h) |
|------------------|---------|------------|-------------|------------|-----------|------------|-----------|-------------------------|------------------------|
| All              | 797     | 0.03       | 29.35       | 313.82     | -70.61    | 6.53       | 313.82    | 820.49                  | -295.38                |
| 0 ≤ GOR < 250    | 210     | 0.43       | 28.95       | 313.82     | -70.61    | 1.28       | 313.82    | 305.52                  | -104.91                |
| 250 ≤ GOR < 550  | 214     | 0.38       | 24.28       | 247.46     | -57.35    | -8.58      | 247.46    | 296.49                  | -194.79                |
| 550 ≤ GOR < 750  | 89      | 0.03       | 24.21       | 81.02      | -62.90    | -6.92      | 81.02     | 84.03                   | -45.46                 |
| 750 ≤ GOR < 1000 | 67      | 0.33       | 21.56       | 209.83     | -64.13    | 1.97       | 209.83    | 41.96                   | -11.37                 |
| GOR ≥ 1000       | 217     | 0.53       | 39.26       | 247.19     | -51.72    | 33.45      | 247.19    | 92.49                   | 61.16                  |

**Table 9** First satellite: results of the Gilbert correlation under the subcritical regime

| Constraint       | Nb data | MinRAE (%) | MeanRAE (%) | MaxRAE (%) | MinRE (%) | MeanRE (%) | MaxRE (%) | SAD (m <sup>3</sup> /h) | SD (m <sup>3</sup> /h) |
|------------------|---------|------------|-------------|------------|-----------|------------|-----------|-------------------------|------------------------|
| All              | 458     | 0.001      | 45.63       | 1419.35    | -79.30    | 26.14      | 1419.35   | 565.79                  | 171.24                 |
| 0 ≤ GOR < 250    | 182     | 0.001      | 41.16       | 288.32     | -46.36    | 29.48      | 288.32    | 254.04                  | 133.96                 |
| 250 ≤ GOR < 550  | 94      | 0.34       | 29.12       | 107.14     | -68.27    | 3.05       | 107.14    | 145.11                  | 1.96                   |
| 550 ≤ GOR < 750  | 49      | 0.74       | 36.67       | 294.79     | -66.03    | 11.92      | 294.79    | 59.28                   | 5.72                   |
| 750 ≤ GOR < 1000 | 30      | 0.57       | 43.42       | 160.63     | -65.94    | 21.07      | 160.63    | 27.83                   | 3.13                   |
| GOR ≥ 1000       | 103     | 1.32       | 73.50       | 1419.35    | -79.30    | 49.56      | 1419.35   | 79.53                   | 26.47                  |

**Table 10** First satellite: results of the revised Gilbert model under the critical regime

| Constraint       | Nb data | a         | b        | c        | MinRAE (%) | MeanRAE (%) | MaxRAE (%) | MinRE (%) | MeanRE (%) | MaxRE (%) | SAD (m <sup>3</sup> /h) | SD (m <sup>3</sup> /h) |
|------------------|---------|-----------|----------|----------|------------|-------------|------------|-----------|------------|-----------|-------------------------|------------------------|
| All              | 797     | 0.068687  | 1.915956 | 0.497091 | 0.11       | 35.13       | 379.59     | -69.32    | 19.97      | 379.59    | 792.55                  | 17.56                  |
| 0 ≤ GOR < 250    | 210     | 0.009240  | 1.676609 | 0.059760 | 0.02       | 22.97       | 290.54     | -60.01    | 6.51       | 290.54    | 252.15                  | -6.47                  |
| 250 ≤ GOR < 550  | 214     | 0.128008  | 1.891906 | 0.559361 | 0.48       | 20.97       | 303.18     | -50.44    | 6.37       | 303.17    | 217.21                  | -8.40                  |
| 550 ≤ GOR < 750  | 89      | 10.585319 | 1.305087 | 0.833976 | 0.13       | 24.32       | 152.77     | -55.92    | 7.57       | 152.77    | 69.80                   | -4.10                  |
| 750 ≤ GOR < 1000 | 67      | 38.903184 | 1.494848 | 1.068230 | 0.32       | 23.22       | 188.97     | -58.22    | 6.87       | 188.97    | 43.58                   | -2.84                  |
| GOR ≥ 1000       | 217     | 1.802409  | 1.696350 | 0.800076 | 0.15       | 21.48       | 136.23     | -59.93    | 5.15       | 136.23    | 67.18                   | -3.02                  |



**Table 11** First satellite: results of the revised Gilbert model under the subcritical regime

| Constraint       | Nb data | a         | b        | c         | MinRAE (%) | MeanRAE (%) | MaxRAE (%) | MinRE (%) | MeanRE (%) | MaxRE (%) | SAD (m <sup>3</sup> /h) | SD (m <sup>3</sup> /h) |
|------------------|---------|-----------|----------|-----------|------------|-------------|------------|-----------|------------|-----------|-------------------------|------------------------|
| All              | 458     | 0.242805  | 1.492394 | 0.475392  | 0.13       | 46.20       | 2037.73    | -75.61    | 24.13      | 2037.73   | 517.27                  | -26.08                 |
| 0 ≤ GOR < 250    | 182     | 0.011859  | 1.685300 | 0.124490  | 0.02       | 29.14       | 286.35     | -53.64    | 11.16      | 286.35    | 199.04                  | -1.35                  |
| 250 ≤ GOR < 550  | 94      | 7.903745  | 0.753316 | 0.540816  | 0.18       | 26.25       | 123.20     | -42.64    | 8.52       | 123.20    | 110.00                  | -1.74                  |
| 550 ≤ GOR < 750  | 49      | 1.257977  | 0.450803 | 0.181977  | 0.51       | 31.37       | 313.04     | -51.11    | 12.88      | 313.04    | 42.13                   | -1.55                  |
| 750 ≤ GOR < 1000 | 30      | 0.101581  | 0.646278 | -0.009659 | 1.96       | 41.40       | 156.60     | -52.80    | 23.65      | 156.60    | 22.38                   | 1.23                   |
| GOR ≥ 1000       | 103     | 42.725399 | 0.675676 | 0.721336  | 0.42       | 46.31       | 403.21     | -70.71    | 23.37      | 403.21    | 47.65                   | -3.63                  |

**Table 12** First satellite: results of extension (2) under the subcritical regime

| Constraint       | Nb data | a          | b        | c        | MinRAE (%) | MeanRAE (%) | MaxRAE (%) | MinRE (%) | MeanRE (%) | MaxRE (%) | SAD (m <sup>3</sup> /h) | SD (m <sup>3</sup> /h) |
|------------------|---------|------------|----------|----------|------------|-------------|------------|-----------|------------|-----------|-------------------------|------------------------|
| All              | 458     | 1.557095   | 1.637518 | 0.557372 | 0.01       | 41.58       | 587.20     | -120.58   | 0.60       | 587.20    | 609.38                  | -202.20                |
| 0 ≤ GOR < 250    | 182     | 0.071139   | 1.910577 | 0.242458 | 0.15       | 36.11       | 198.38     | -122.43   | -9.82      | 198.38    | 273.92                  | -105.63                |
| 250 ≤ GOR < 550  | 94      | 4.447270   | 1.086794 | 0.409563 | 0.74       | 31.15       | 144.22     | -72.67    | -4.52      | 144.22    | 136.82                  | -39.32                 |
| 550 ≤ GOR < 750  | 49      | 118.509645 | 0.900509 | 0.724599 | 1.94       | 33.23       | 124.15     | -86.60    | -0.51      | 124.15    | 52.57                   | -15.49                 |
| 750 ≤ GOR < 1000 | 30      | 268.684655 | 1.483165 | 1.091019 | 0.02       | 36.60       | 183.70     | -68.50    | 5.87       | 183.70    | 24.26                   | -4.34                  |
| GOR ≥ 1000       | 103     | 235.017966 | 0.745515 | 0.748169 | 1.01       | 42.96       | 174.52     | -93.29    | 1.51       | 174.52    | 56.83                   | -20.61                 |

**Table 13** First satellite: results of extension (3) under the subcritical regime

| Constraint       | Nb data | <i>a</i>  | <i>b</i> | <i>c</i> | <i>d</i>  | MinRAE (%) | MeanRAE (%) | MaxRAE (%) | MinRE (%) | MeanRE (%) | MaxRE (%) | SAD (m <sup>3</sup> /h) | SD (m <sup>3</sup> /h) |
|------------------|---------|-----------|----------|----------|-----------|------------|-------------|------------|-----------|------------|-----------|-------------------------|------------------------|
| All              | 458     | 0.200959  | 1.524972 | 0.498714 | -1.412215 | 0.10       | 41.98       | 1553.28    | -73.97    | 20.28      | 1553.28   | 487.11                  | -31.68                 |
| 0 ≤ GOR < 250    | 182     | 0.009703  | 1.731297 | 0.152043 | -1.349534 | 0.03       | 26.38       | 271.95     | -57.82    | 9.02       | 271.95    | 182.41                  | -3.92                  |
| 250 ≤ GOR < 550  | 94      | 3.723146  | 0.832017 | 0.511876 | -1.208508 | 0.42       | 25.30       | 114.88     | -44.17    | 6.99       | 114.88    | 106.45                  | -3.57                  |
| 550 ≤ GOR < 750  | 49      | 1.366568  | 0.544525 | 0.264143 | -1.395251 | 0.33       | 29.76       | 272.20     | -56.47    | 11.64      | 272.20    | 40.44                   | -1.77                  |
| 750 ≤ GOR < 1000 | 30      | 1.256572  | 0.810444 | 0.389131 | -1.282446 | 1.28       | 37.67       | 163.38     | -54.19    | 20.47      | 163.38    | 21.32                   | 0.78                   |
| GOR ≥ 1000       | 103     | 39.102300 | 0.675764 | 0.726760 | -0.761628 | 0.15       | 44.99       | 358.86     | -69.11    | 21.60      | 358.86    | 47.35                   | -4.13                  |

**Table 14** First satellite: results of extension (4) under the subcritical regime

| Constraint       | Nb data | <i>a</i>  | <i>b</i> | <i>c</i> | MinRAE (%) | MeanRAE (%) | MaxRAE (%) | MinRE (%) | MeanRE (%) | MaxRE (%) | SAD (m <sup>3</sup> /h) | SD (m <sup>3</sup> /h) |
|------------------|---------|-----------|----------|----------|------------|-------------|------------|-----------|------------|-----------|-------------------------|------------------------|
| All              | 458     | 0.347591  | 1.529117 | 0.515009 | 0.11       | 39.94       | 1239.21    | 0.07      | 15.62      | 1239.20   | 488.68                  | -60.28                 |
| 0 ≤ GOR < 250    | 182     | 0.014777  | 1.757892 | 0.163346 | 0.36       | 25.89       | 270.73     | -0.36     | 3.88       | 270.73    | 178.98                  | -23.74                 |
| 250 ≤ GOR < 550  | 94      | 4.701726  | 0.883541 | 0.517708 | 0.90       | 24.58       | 122.42     | -51.65    | 4.49       | 122.42    | 106.11                  | -8.57                  |
| 550 ≤ GOR < 750  | 49      | 3.035513  | 0.621142 | 0.344332 | 0.77       | 29.40       | 233.67     | -69.58    | 9.25       | 233.66    | 41.30                   | -4.07                  |
| 750 ≤ GOR < 1000 | 30      | 24.235699 | 0.919326 | 0.738527 | 3.63       | 34.71       | 166.43     | -54.32    | 16.61      | 166.43    | 21.09                   | 0.07                   |
| GOR ≥ 1000       | 103     | 63.900028 | 0.663111 | 0.742040 | 0.11       | 42.73       | 255.01     | -78.63    | 15.48      | 255.01    | 48.65                   | -8.09                  |



## References

- Guo, B.; Lyons, W.C.; Ghalambor, A.: Petroleum Production Engineering: A Computer-Assisted Approach. Gulf Professional Publishing, Burlington (2007)
- Sachdeva, R.; Schmidt, Z.; Brill, J.P.; Blais, R.M.: Two-phase flow through chokes. In: The SPE Annual Technical Conference and Exhibition, New Orleans, 5–8 October (1986)
- Seidi, S.; Sayahi, T.: A new correlation for prediction of sub-critical two-phase flow pressure drop through large-sized wellhead chokes. *J. Nat. Gas Sci. Eng.* **26**, 264–278 (2015)
- Babelli, I.M.M.: In search of an ideal multiphase flow meter for the oil industry. *Arab. J. Sci. Eng.* **27**(2), 113–126 (2002)
- Thorn, R.; Johansen, G.A.; Hjertaker, B.T.: Three-phase flow measurement in the petroleum industry. *Meas. Sci. Technol.* **24**(1), 012003 (2012)
- Mwalyepelo, J.; Stanko, M.: Improvement of multiphase flow rate model for chokes. *J. Pet. Sci. Eng.* **145**, 321–327 (2016)
- Shao, H.; Jiang, L.; Liu, L.; Zhao, O.: Modeling of multiphase flow through chokes. *Flow Meas. Instrum.* **60**, 44–50 (2018)
- Choubineh, A.; Ghorbani, H.; Wood, D.A.; RobabMoosavi, S.; Khalafi, E.; Sadatshojaei, E.: Improved predictions of wellhead choke liquid critical-flow rates: modelling based on hybrid neural network training learning based optimization. *Fuel* **207**, 547–560 (2017)
- Gilbert, W.E.: Flowing and gas-lift well performance. *API Drill. Prod. Pract.* **20**, 126–157 (1954)
- Tangren, R.F.; Dodge, C.H.; Seifert, H.S.: Compressibility effects in two-phase flow. *J. Appl. Phys.* **20**(7), 637–645 (1949)
- Ros, N.C.J.: An analysis of critical simultaneous gas/liquid flow through a restriction and its application to flowmetering. *Appl. Sci. Res.* **9**(Section A), 374–388 (1960)
- Poettmann, F.E.; Beck, R.L.: New charts developed to predict gas-liquid flow through chokes. *Word Oil* **184**(3), 95–100 (1963)
- Omana, R.A.: Multiphase flow through chokes. M.S. Thesis, University of Tulsa (1968)
- Ashford, F.E.; Pierce, P.E.: Determining multiphase pressure drops and flow capacities in down-hole safety valves. *J. Pet. Technol.* **27**(9), 1145–1152 (1975)
- Perkins, T.K.: Critical and subcritical flow of multiphase mixtures through chokes. *SPE Drill. Complet.* **8**(4), 271–276 (1993)
- Al-Safran, E.M.; Kelkar, M.G.: Predictions of two-phase critical flow boundary and mass flow rate across chokes. *SPE Prod. Oper.* **24**, 249–256 (2009)
- Selmer-Olsen, S.; Holm, H.; Haugen, K.; Nilsen, P.; Sandberg, R.: Subsea chokes as multiphase flowmeters: production control at troll olje. In: Proceedings of the BHR Group 7th International Conference on Multiphase Production, Cannes, France, 7–9 June (1995)
- Schüller, R.B.; Solbakken, T.; Selmer-Olsen, S.: Evaluation of multiphase flow rate models for chokes under subcritical oil/gas/water flow conditions. *SPE Prod. Facil.* **18**(3), 170–181 (2003)
- Schüller, R.B.; Munawera, S.; Selmer-Olsen, S.; Solbakken, T.: Critical and subcritical oil/gas/water mass flow rate experiments and predictions for chokes. *SPE Prod. Oper.* **21**(3), 372–380 (2006)
- Rastoin, S.; Schmidt, Z.; Doty, D.R.: A review of multiphase flow through chokes. *J. Energy Res. Technol.* **119**(1), 1–10 (1997)
- Al-Attar, H.H.; Abdul-Majeed, G.H.: Revised bean performance equation for east Baghdad oil wells. *SPE Prod. Eng.* **3**(1), 127–131 (1988)
- Ashford, F.E.: An evaluation of critical multiphase flow performance through wellhead chokes. *J. Pet. Technol.* **26**(8), 843–850 (1974)
- Abdul-Majeed, G.H.; Maha, R.A.A.: Correlations developed to predict two-phase flow through wellhead chokes. *J. Can. Pet. Technol.* **30**(06), 47–55 (1991)
- Achong, I.: Revised bean performance formula for lake maracaibo wells. Internal Company Report, Shell Oil Co., Houston, TX (1961)
- Elgibaly, A.A.M.; Nashawi, I.S.: New correlations for critical and subcritical two-phase flow through wellhead chokes. *J. Can. Pet. Technol.* **37**(06), 36–43 (1998)
- Abdul-Majeed, G.H.; Aswad, Z.A.: A new approach for estimating the orifice discharge coefficient required in the Ashford–Pierce correlation. *J. Pet. Sci. Eng.* **5**(1), 25–33 (1990)
- Al-Marhoun, M.A.: Pvt correlations for middle east crude oils. *J. Pet. Technol.* **40**(05), 650–666 (1988)
- Dranchuk, P.M.; Purvis, R.A.; Robinson, D.B.: Computer calculation of natural gas compressibility factors using the standing and Katz correlation. In: Annual Technical Meeting, Edmonton, May 8–12 (1973)
- Mirzaei-Paiaman, A.; Salavati, S.: A new empirical correlation for sonic simultaneous flow of oil and gas through wellhead chokes for Persian oil fields. *Energy Sour., Part A: Recover., Util., Environ. Eff.* **35**(9), 817–825 (2013)
- Baxendell, P.B.: Bean performance-lake wells. Shell Internal Report (1957)
- Pilehvari, A.A.: Experimental study of critical two-phase flow through wellhead chokes. Fluid Flow Projects Report, University of Tulsa (1981)
- Fortunati, F.: Two-phase flow through wellhead chokes. In: SPE European Spring Meeting, Amsterdam, Netherlands, 16–18 May (1972)
- Surbey, D.W.; Kelkar, B.G.; Brill, J.P.: Study of multiphase critical flow through wellhead chokes. *SPE Prod. Eng.* **4**(02), 142–146 (1989)
- Al-Attar, H.H.: Performance of wellhead chokes during sub-critical flow of gas condensates. *J. Pet. Sci. Eng.* **60**(3), 205–212 (2008)
- AlAjmi, M.D.; Alarifi, S.A.; Mahsoon, A.H.: Improving multiphase choke performance prediction and well production test validation using artificial intelligence: a new milestone. In: SPE Digital Energy Conference and Exhibition, TX, USA, 3–5 March (2015)
- Nasriani, H.R.; Kalantariasl, A.: Choke performance in high-rate gas condensate wells under subcritical flow condition. *Energy Sour., Part A: Recover., Util., Environ. Eff.* **37**(2), 192–199 (2015)
- Ghorbani, H.; Wood, D.A.; Moghadasi, J.; Choubineh, A.; Abdizadeh, P.; Mohamadian, N.: Predicting liquid flow-rate performance through wellhead chokes with genetic and solver optimizers: an oil field case study. *J. Pet. Exp. Prod. Technol.* **9**, 1355–1373 (2019)
- Safar Beiranvand, M.; Mohammadmoradi, P.; Aminshahidy, B.; Fazelabdolabadi, B.; Aghahoseini, S.: New multiphase choke correlations for a high flow rate Iranian oil field. *Mech. Sci.* **3**(1), 43–47 (2012)
- Mirzaei-Paiaman, A.; Salavati, S.: The application of artificial neural networks for the prediction of oil production flow rate. *Energy Sour., Part A: Recover., Util., Environ. Eff.* **34**(19), 1834–1843 (2012)
- Levenberg, K.: A method for the solution of certain non-linear problems in least squares. *Q. Appl. Math.* **2**(2), 164–168 (1944)
- Marquardt, D.W.: An algorithm for least-squares estimation of non-linear parameters. *J. Soc. Ind. Appl. Math.* **11**(2), 431–441 (1963)
- Smyth, G.K.: Nonlinear regression. *Encycl. Environ.* **4**, 1405–1411 (2002)
- Murthy, Z.V.P.: Nonlinear Regression: Levenberg–Marquardt Method, pp. 1–3. Springer, Berlin, Heidelberg (2015)